Spin Waves and Magnetic Resonance in Rare-Earth Metals: Thermal, Applied-Field, and Magnetoelastic Effects

BERNARD R. COOPER
General Electric Research and Development Center, Schenectady, New York
(Received 22 November 1967)

The theory is developed for the temperature and magnetic field dependence expected for the energy of long-wavelength spin waves in ferromagnetic heavy rare-earth metals. Emphasis is placed on examining magnetoelastic effects on the spin-wave energies. The resulting theory is applied to understanding recent neutron inelastic-scattering and ferromagnetic-resonance experiments in Tb and Dy. For Tb and Dy, comparison of theoretical predictions with the experimental results, especially the magnetic field dependence of the uniform-mode spin-wave energy, precludes the applicability of the frozen-lattice approximation suggested by Turov and Shavrov for magnetoelastic effects on spin-wave energies. The most striking point found in the present work is the contrast between the behavior of Tb and that of Dy. For Tb, the magnitude of the planar anisotropy constant found in static measurements is much smaller than the value necessary for agreement with the spin-wave experiments, i.e., neutron inelastic scattering and ferromagnetic resonance, which are mutually consistent. In contrast to this puzzling discrepancy for Tb, for Dy the static measured planar anisotropy constant gives absolute calculated values for the spin-wave behavior in excellent agreement with the results of ferromagnetic-resonance experiments.

1. INTRODUCTION

EARLIER studies[1,2] have treated the nature of spin-wave excitations in the heavy rare-earth metals. These studies, however, did not discuss the temperature dependence of the spin-wave energies in any detail, nor did they include magnetoelastic effects. The present paper is intended to include such effects for long-wavelength spin waves in the ferromagnetic regime, and to apply the resulting theory to understanding the relevant recent experimental results. The relevant experiments are neutron inelastic scattering for Tb and ferromagnetic resonance for both Tb and Dy. Since applied-field effects on the ferromagnetic spin waves play an important role in separating out and understanding the various effects present, they are treated in somewhat more detail than in the previous work.[1]

In a recent note[3] we have pointed out the importance of magnetoelastic effects for understanding both the equilibrium and excited-state magnetic properties of rare-earth metals. It was shown that the driving force for the spiral to ferromagnetic transition in Dy and Tb is the energy of cylindrical symmetry associated with the lowest-order magnetostriction effects. We also briefly mentioned the expected effect of magnetoelastic forces on the spin-wave energies. These ideas are treated in more detail in the present note. In particular, we show that for both Tb and Dy results of neutron inelastic scattering (done for Tb only) and ferromagnetic-resonance experiments preclude the applicability of the frozen-lattice approximation suggested by Turov and Shavrov[4] for treating magnetoelastic effects on spin-wave energies. Turov and Shavrov suggested that the correct way to find the uniform-mode frequency is to regard the strain as frozen at its equilibrium position. Then, in the excited state, the relative orientation of moment and strain changes, and there is a net increase of energy relative to the equilibrium state, even though the equilibrium energy associated with the magnetostriction has cylindrical symmetry. However, comparison of the results of the present detailed calculations with experiment, as discussed below, suggests, to the contrary, that the strains move with the motion of the magnetization for the long-wavelength modes.

The most striking point found in the present work is the contrast between the behavior of Tb and that of Dy. For Tb the magnitude of the planar anisotropy constant found in static measurements[5] is much smaller than the value necessary for agreement with the spin-wave experiments, i.e., neutron inelastic scattering[6,7,7a] and ferromagnetic resonance[8] which are mutually consistent. (This discrepancy in magnitude of the planar anisotropy has already been pointed out by Møller *et al.*[6] for the neutron inelastic scattering experiments.) If the frozen-lattice approximation were applicable, the spin-wave energies would be larger than those expected using the value of the static planar anisotropy constant and not including any frozen-lattice effects. This is true because when the frozen-lattice approximation applies, the lowest-order energy

[1] B. R. Cooper, R. J. Elliott, S. J. Nettel, and H. Suhl, Phys. Rev. **127**, 57 (1962). Referred to as I in the text.
[2] B. R. Cooper and R. J. Elliott, Phys. Rev. **131**, 1043 (1963); **153**, 654(E) (1967).
[3] B. R. Cooper, Phys. Rev. Letters **19**, 900 (1967).
[4] E. A. Turov and V. G. Shavrov, Fiz. Tverd. Tela **7**, 217 (1965) [English transl.: Soviet Phys.—Solid State **7**, 166 (1965)].
[5] J. J. Rhyne and A. E. Clark, J. Appl. Phys. **38**, 1379 (1967).
[6] H. Bjerrum Møller, J. C. Gylden Houmann, and A. R. Mackintosh, Phys. Rev. Letters **19**, 312 (1967).
[7] H. Bjerrum Møller, J. C. Gylden Houmann, and A. R. Mackintosh, Sixth Rare Earth Conference, Gatlinburg, Tennessee, 1967 (unpublished).
[7a] H. Bjerrum Møller, J. C. Gylden Houmann, and A. R. Mackintosh, J. Appl. Phys. **39**, 807 (1968).
[8] D. M. S. Bagguley and J. Liesegang, J. Appl. Phys. **37**, 1220 (1966); Proc. Roy. Soc. (London) **A300**, 497 (1967).

associated with magnetostriction (of cylindrical symmetry) would contribute to the spin-wave energy, but not to the static planar anisotropy constant. However, the experimental temperature and field dependence of the spin-wave behavior rules out the applicability of the frozen-lattice approximation.

In contrast to the puzzling discrepancy with regard to size of planar anisotropy which occurs for Tb, for Dy the static measured anisotropy constant[5,9] gives absolute calculated values for the spin-wave behavior in excellent agreement with the results of ferromagnetic-resonance experiments.[10,11] Moreover, the detailed temperature dependence of the resonance field in Dy is in excellent agreement with theory when the frozen-lattice approximation is inapplicable. Thus, once one decides that the frozen-lattice approximation does not apply, the absolute agreement between theory and experiment for the spin-wave behavior in dysprosium is excellent.

2. TEMPERATURE AND FIELD DEPENDENCE OF SPIN-WAVE ENERGIES FOR FERROMAGNETIC HEAVY RARE EARTHS

We begin our detailed discussion by generalizing the results of Cooper *et al.*[1] (referred to as I hereafter) to include the temperature dependence of the spin-wave energies. We also give a more complete description of applied-field effects than is found in I.

We discuss the spin-wave excitations for a ferromagnetic system characterized by the following Hamiltonian:

$$\mathcal{H}=-\sum_{i\neq j} J_{ij}\mathbf{S}_i\cdot\mathbf{S}_j-\sum_i\{P_2S_{i\zeta}{}^2-\tfrac{1}{2}P_6{}^6\times[(S_{i\xi}+iS_{i\eta})^6+(S_{i\xi}-iS_{i\eta})^6]\}. \quad (2.1)$$

Here and throughout this paper S denotes total angular momentum, spin+orbital—the usual J. There is an exchange term of a long-range, oscillatory character, a large axial anisotropy term which guarantees that the equilibrium magnetic arrangement is planar, and a hexagonal planar anisotropy term. The easy direction for the planar anisotropy is taken as the ξ axis; and in the absence of an applied magnetic field the ferromagnetic alignment is in that direction. With the further inclusion of magnetoelastic effects, to be discussed below, this Hamiltonian quite adequately describes the behavior of Dy and Tb in the ferromagnetic regimes. (As shown in I to lowest order in $1/S$, i.e., neglecting zero-point motion effects, higher-order axial-anisotropy terms do not contribute to the spin-wave energies when the equilibrium magnetic arrangement is ferromagnetic alignment in the planes perpendicular to the c axis.)

As shown in I, it is a straightforward procedure, taking a coordinate system with the z axis along ξ and using the standard Holstein-Primakoff transformation technique, to find the spin-wave energies for the Hamiltonian of (2.1). These are

$$\hbar\omega(\mathbf{q})=S^{-1}\{[-2P_2S^2+2S^2J(0)-2S^2J(\mathbf{q})-6P_6{}^6S^6]\times[2S^2J(0)-2S^2J(\mathbf{q})-36P_6{}^6S^6]\}^{1/2}, \quad (2.2)$$

with

$$J(\mathbf{q})\equiv\sum_j J_{ij}\exp[i\mathbf{q}\cdot(\mathbf{R}_i-\mathbf{R}_j)]. \quad (2.2')$$

This then gives the spin-wave dispersion law at $T=0$ for a ferromagnetic arrangement along the planar easy axis as in Dy or Tb. (The treatment of I, and that of the present paper, treats the hcp lattice as a Bravais lattice. This gives the correct results for the acoustic spin waves which are of interest to us, and actually gives the exact result for all energies for $\mathbf{q}$ parallel to the c axis. The hcp lattice is not a Bravais lattice, so that the spin-wave spectrum strictly speaking has two branches, an acoustic and an optical branch. Niira[12] treated this problem by considering two interpenetrating hexagonal Bravais lattices.) The expression in (2.2) neglects terms from the P_2 and $P_6{}^6$ contributions arising from commuting spin operators for the same site. Such terms go as $1/S$ compared with the retained terms and thus are expected to give small contributions, i.e., $S=\frac{15}{2}$ for Dy, $S=6$ for Tb.

The spin-wave dispersion law given by (2.2) holds at $T=0$. It is a simple matter, however, to see approximately how the spin-wave energies should decrease with increasing temperature. This is most easily done by using an approximation regarding the renormalization of the anisotropy parts at low energy (long wavelengths) and that of the exchange part at high energies separately.

The renormalization of the anisotropy terms is accomplished by considering the phenomenological macroscopic theory developed by Smit[13,14] for treating ferromagnetic resonance in highly anisotropic materials. That theory determines the resonance frequency and its temperature dependence. The ferromagnetic-resonance frequency is the frequency of the $\mathbf{q}=0$ mode, and the particular renormalization arrived at is appropriate for long-wavelength spin waves. The anisotropy terms in (2.1) correspond to a free energy of the form

$$F=K_2(T)\sin^2\theta+K_6(T)\sin^6\theta\cos6\phi, \quad (2.3)$$

where K_2 and K_6 are the macroscopic temperature-dependent anisotropy constants. Then the frequency of the $\mathbf{q}=0$ mode is given by

$$\hbar\omega(0)=(g\beta/M)(F_{\theta\theta}F_{\phi\phi}-F_{\theta\phi}{}^2)^{1/2}, \quad (2.4)$$

[9] S. H. Liu, D. R. Behrendt, S. Legvold, and R. H. Good, Jr., Phys. Rev. **116**, 1464 (1959).
[10] F. C. Rossol and R. V. Jones, J. Appl. Phys. **37**, 1227 (1966).
[11] F. C. Rossol, Ph.D. thesis, Harvard University, 1966 (unpublished).
[12] K. Niira, Phys. Rev. **117**, 129 (1960).
[13] J. Smit and H. G. Beljers, Philips Res. Rept. **10**, 113 (1955).
[14] J. Smit and H. P. J. Wijn, *Ferrites* (John Wiley & Sons, Inc., New York, 1959), Chap. 6.

where g is the Lande factor, β is the Bohr magneton, M is the magnetization, and $F_{\theta\theta}$, etc., denote second derivatives of the energy with respect to angle evaluated at the equilibrium position, $\theta=\frac{1}{2}\pi$, $\phi=0$.

$$F_{\theta\theta}\equiv\partial^2F/\partial\theta^2. \tag{2.5}$$

This gives

$$\hbar\omega(0)=(g\beta/M)\{[2K_2(T)+6K_6(T)][36K_6(T)]\}^{1/2}. \tag{2.6}$$

The temperature dependence of $\hbar\omega(0)$ can be introduced explicitly into (2.6) in terms of the reduced magnetization using the theory of Callen and Callen[15] for the temperature dependence of the macroscopic anisotropy constants.

$$\hbar\omega(0)=(g\beta/M)\{(2K_2(0)\hat{I}_{5/2}[\mathfrak{L}^{-1}(\sigma)]+6K_6(0)\times\hat{I}_{13/2}[\mathfrak{L}^{-1}(\sigma)])(36K_6(0)\hat{I}_{13/2}[\mathfrak{L}^{-1}(\sigma)])\}^{1/2}. \tag{2.7}$$

Here, $\hat{I}_{(2l+1)/2}[\mathfrak{L}^{-1}(\sigma)]$ is the ratio of hyperbolic Bessel function of order $\frac{1}{2}(2l+1)$ to that of order $\frac{1}{2}$, where the argument of the Bessel functions is the inverse Langevin function of the reduced magnetization. For low T, $\hat{I}_{(2l+1)/2}$ goes as $\sigma^{l(l+1)/2}$; while as $m\to0$, $\hat{I}_{(2l+1)/2}$ goes as σ^l. Actually, the low T, $\sigma^{l(l+1)/2}$, approximation is usually good for most of the ordered temperature range.

Then by comparison with (2.2) the temperature renormalization of $\hbar\omega(\mathbf{q})$ in the limit $\mathbf{q}\to0$ is clear.

$$\hbar\omega(0)=(\sigma S)^{-1}\{(-2P_2S^2\hat{I}_{5/2}[\mathfrak{L}^{-1}(\sigma)]-6P_6{}^6S^6\times\hat{I}_{13/2}[\mathfrak{L}^{-1}(\sigma)])(-36P_6{}^6S^6\hat{I}_{13/2}[\mathfrak{L}^{-1}(\sigma)])\}^{1/2}. \tag{2.8}$$

Thus, the anisotropy terms in the spin-wave energy are renormalized as the corresponding anisotropy field, i.e., as the corresponding anisotropy energy divided by magnetization. Liesegang[16] used such a renormalization scheme in discussing his resonance results (although the correct dependence of anisotropy energy on reduced magnetization was not used); and Møller *et al.*[6,7] have also used an equivalent scheme for discussing their neutron inelastic scattering in Tb.

The simplest, reasonably accurate way to renormalize the exchange contribution in (2.2) is to use the random phase approximation (RPA), and multiply the exchange-energy terms by a factor σ^2.

$$\hbar\omega(\mathbf{q})=(\sigma S)^{-1}\{(-2P_2S^2\hat{I}_{5/2}[\mathfrak{L}^{-1}(\sigma)]+2\sigma^2S^2[J(0)-J(\mathbf{q})]-6P_6{}^6S^6\hat{I}_{13/2}[\mathfrak{L}^{-1}(\sigma)])(2\sigma^2S^2[J(0)-J(\mathbf{q})]-36P_6{}^6S^6\hat{I}_{13/2}[\mathfrak{L}^{-1}(\sigma)])\}^{1/2}. \tag{2.9}$$

As the anisotropy terms vanish, the RPA gives spin-wave energies renormalized proportionally to the reduced magnetization. The RPA approximation is accurate in the high-energy limit. Thus, this simple approximation should be accurate both at low energies where the anisotropy terms dominate and have been correctly normalized as $\mathbf{q}\to0$, and at high energies where exchange dominates and is properly normalized by the RPA. A renormalization scheme equivalent to this was used to discuss the spin-wave spectrum for Tb by Møller *et al.*[6,7]

Now, following the treatment of I, we consider the effect of an applied magnetic field on the spin waves. For field parallel to the easy axis, the spin-wave frequency simply increases monotonically with applied field. Then the spin-wave frequency of (2.2) becomes

$$\hbar\omega(\mathbf{q})=\{(-2P_2S[\hat{I}_{5/2}/\sigma]+2\sigma S[J(0)-J(\mathbf{q})]-6P_6{}^6S^5[\hat{I}_{13/2}/\sigma]+g\beta H)(2\sigma S[J(0)-J(\mathbf{q})]-36P_6{}^6S^5[\hat{I}_{13/2}/\sigma]+g\beta H)\}^{1/2}. \tag{2.10}$$

Here we adopt the convention used through the remainder of this paper, that whenever $\hat{I}_{(2l+1)/2}$ appears, the argument is understood to be $\mathfrak{L}^{-1}(\sigma)$.

For the $\mathbf{q}=0$, uniform mode observed in ferromagnetic resonance, the appropriate demagnetizing fields should also be included:

$$\hbar\omega(0)=\{(-2P_2S[\hat{I}_{5/2}/\sigma]-6P_6{}^6S^5[\hat{I}_{13/2}/\sigma]+g\beta[H-(N_\xi-N_\zeta)M])\times(-36P_6{}^6S^5[\hat{I}_{13/2}/\sigma]+g\beta[H-(N_\xi-N_\eta)M])\}^{1/2}. \tag{2.11}$$

Here N_ξ, N_η, and N_ζ are the demagnetizing factors along the three axes. In (2.11) we note that the sign of the demagnetizing factor has been corrected from that given in (8.8) of I. With our sign conventions, P_2 and $P_6{}^6$ are negative (i.e., ξ is an a axis for Dy and a b axis for Tb), while g and the N_i are positive. In practice, one can usually perform the experiments in such a way that demagnetizing effects can be neglected. The demagnetizing factor along the c axis, N_ζ, appears only in the factor where the very large effective axial anisotropy field appears. In this factor all applied-field effects can usually be safely neglected. On the other hand, the demagnetizing factors in the plane, N_ξ and N_η, can usually be made negligible by using a sample in the form of a thin disk with the c axis as normal.

The effect of an applied field along a hard planar axis as treated in I is much more interesting than that for a field along an easy axis. Such an applied field pulls the magnetization away from the easy axis. The Hamiltonian for this system is

$$\mathcal{H}=-\sum_{i\neq j}J_{ij}\mathbf{S}_i\cdot\mathbf{S}_j-P_2\sum_i S_{i\zeta}{}^2+\tfrac{1}{2}P_6{}^6\sum_i[(S_{i\xi}+iS_{i\eta})^6+(S_{i\xi}-iS_{i\eta})^6]-g\beta H\cos\tfrac{1}{6}\pi\sum_i S_{i\xi}-g\beta H\sin\tfrac{1}{6}\pi\sum_i S_{i\eta}. \tag{2.12}$$

The effect on the spin waves as the magnetization moves toward a hard axis can be seen by transforming

[15] H. B. Callen and E. Callen, J. Phys. Chem. Solids **27**, 1271 (1966).

[16] J. Liesegang, D. Phil. thesis, University of Oxford, 1966 (unpublished).

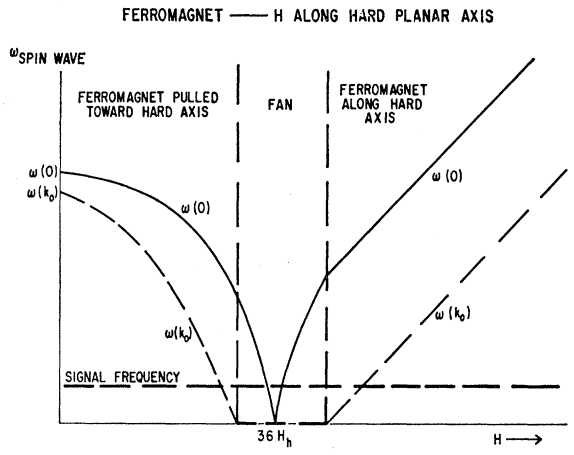

FIG. 1. Field variation of $\omega(0)$ and $\omega(k_0)$ for ferromagnet with H along the hard planar axis. $H_h=-P_6{}^6S^5I_{13/2}/g\beta\sigma$.

to a coordinate system with z axis along the equilibrium-magnetization direction for the applied field.[1]

$$x=-\zeta,$$
$$y=-\xi\sin\delta+\eta\cos\delta,$$
$$z=\xi\cos\delta+\eta\sin\delta. \tag{2.13}$$

Here δ (the angle between the direction of magnetization and the easy axis) is determined by the condition that the equilibrium energy be minimized.

$$0=-6P_6{}^6S^6\hat{I}_{13/2}\sin6\delta+g\beta HS\sigma\sin(\delta-\tfrac{1}{6}\pi), \tag{2.14}$$

or with

$$\psi=\tfrac{1}{6}\pi-\delta \tag{2.15}$$

this becomes

$$0=-12P_6{}^6S^6\hat{I}_{13/2}(-1+4\cos^2\psi)(4\cos^3\psi-3\cos\psi)$$
$$-g\beta HS\sigma \tag{2.16}$$

so that $\delta=\frac{1}{6}\pi$, and alignment along the hard axis occurs for $H=36H_h$, where

$$H_h=-P_6{}^6S^5\hat{I}_{13/2}/g\beta\sigma \tag{2.17}$$

is a convenient notation used below.

Using the transformation of (2.13), it is a simple matter to find the Hamiltonian correct to quadratic terms in S_{ix} and S_{iy}. The diagonalization of the Hamiltonian then proceeds in the usual manner. This gives

$$\hbar\omega(\mathbf{q})=\{(2S\sigma[J(0)-J(\mathbf{q})]-2P_2S(\hat{I}_{5/2}/\sigma)$$
$$-6P_6{}^6S^5\cos6\delta(\hat{I}_{13/2}/\sigma)+g\beta H\cos(\tfrac{1}{6}\pi-\delta))$$
$$\times(2S\sigma[J(0)-J(\mathbf{q})]-36P_6{}^6S^5\cos6\delta(\hat{I}_{13/2}/\sigma)$$
$$+g\beta H\cos(\tfrac{1}{6}\pi-\delta))\}^{1/2}. \tag{2.18}$$

We see that $\omega(0)=0$ for $H=36\,H_h$. That is, $\omega(0)$ goes to zero just when the moment is pulled fully around to the hard axis. Actually, for a field slightly less than this, $\omega(\mathbf{k}_0)$ goes to zero and the spin arrangement flops to a fan centered about the hard axis. [This is assuming that the exchange energy itself favors a spiral so that the maximum of $J(\mathbf{q})$ is at $\mathbf{q}=\mathbf{k}_0$.] The behavior of the uniform-mode spin wave is then as shown in Fig. 1. As field increases still further above $36H_h$, $\omega(0)$ increases from zero and the fan closes up to a ferromagnet aligned along the hard axis.

In Fig. 1 the situation corresponding to a relatively low signal frequency is also indicated. Ferromagnetic resonance occurs when the signal frequency matches the frequency of the $\omega(0)$ mode. Thus, for low frequencies (less than 30 GHz, say) one expects to observe resonance for fields near $36H_h$. As the signal frequency increases, one should in principle observe two resonances on either side of $36H_h$, although the lower field resonance may be lost among domain alignment effects. Finally, at high signal frequencies, one should observe only a single high field resonance.

3. MAGNETOELASTIC EFFECTS AND EQUILIBRIUM STRAINS

As already briefly discussed by the present author,[3] in addition to the exchange and anisotropy terms already treated in Sec. 2, a third type of energy contribution is quite important for understanding the magnetic behavior of the system of tripositive rare-earth ions having localized moments. This is the energy associated with magnetostriction effects. Then the Hamiltonian for the spin system is

$$\mathcal{H}=\mathcal{H}_{\rm EX}+\mathcal{H}_{\rm CF}+\mathcal{H}_{\rm MS}. \tag{3.1}$$

Here $\mathcal{H}_{\rm EX}$ and $\mathcal{H}_{\rm CF}$ are the exchange and crystal-field anisotropy terms, respectively, as already given in Sec. 2.

The third term, $\mathcal{H}_{\rm MS}$, comes from magnetostriction effects arising from the modulation by the strain of the crystal-field splittings. [The presence of an applied field, of course, adds a fourth term, the Zeeman energy, to (3.1).]

$$\mathcal{H}_{\rm MS}=\mathcal{H}_{\rm E}+\mathcal{H}_{\rm M}. \tag{3.2}$$

Here $\mathcal{H}_{\rm E}$ is the elastic energy associated with the homogeneous strain components, and $\mathcal{H}_{\rm M}$ is the magnetoelastic interaction, coupling the spin system to the strains.

We have already mentioned in a brief note[3] that the driving force for the spiral to ferromagnetic transition in Dy and Tb is the energy of cylindrical symmetry associated with the lowest-order magnetostriction effects. Basically, the spiral arrangement serves to restrain ("clamp") each successive plane along the c axis from developing the strain that would minimize the combined elastic and magnetoelastic energy. Transition to a ferromagnet allows such energetically favorable strains to develop. We now present this treatment in more detail than was possible in our previous brief communication. This treatment will

also have the benefit of introducing the notation used in discussing magnetoelastic effects on the spin-wave energies.

Accordingly, we treat the magnetostriction contribution to the free energy for a hexagonal crystal. We follow the general treatment of magnetostriction by Callen and Callen[17] and adopt their notation.

The total strain-dependent energy density E_{MS} leading to the magnetostriction is

$$E_{MS}=E_E+E_M, \tag{3.3}$$

where E_E is the elastic contribution and E_M is the magnetoelastic contribution.

The elastic contribution to the free-energy density is of the form

$$E_E=\tfrac{1}{2}c_1^{\alpha}(\epsilon^{\alpha,1})^2+\tfrac{1}{2}c_2^{\alpha}(\epsilon^{\alpha,2})^2+c_{12}^{\alpha}\epsilon^{\alpha,1}\epsilon^{\alpha,2}+\tfrac{1}{2}c^{\gamma}[(\epsilon_1^{\gamma})^2+(\epsilon_2^{\gamma})^2]+\tfrac{1}{2}c^{\epsilon}[(\epsilon_1^{\epsilon})^2+(\epsilon_2^{\epsilon})^2] \tag{3.4}$$

and the magnetoelastic contribution is of the form

$$-E_M=B_1^{\alpha,0}\epsilon^{\alpha,1}+B_2^{\alpha,0}\epsilon^{\alpha,2}+B_1^{\alpha,2}\epsilon^{\alpha,1}(\alpha_\zeta^2-\tfrac{1}{3})+B_2^{\alpha,2}\epsilon^{\alpha,2}(\alpha_\zeta^2-\tfrac{1}{3})+B^{\gamma,2}\epsilon_1^{\gamma}\tfrac{1}{2}(\alpha_\xi^2-\alpha_\eta^2)+B^{\gamma,2}\epsilon_2^{\gamma}\alpha_\xi\alpha_\eta+B^{\epsilon,2}\epsilon_1^{\epsilon}\alpha_\eta\alpha_\zeta+B^{\epsilon,2}\epsilon_2^{\epsilon}\alpha_\zeta\alpha_\xi. \tag{3.5}$$

This includes the lowest-order magnetoelastic effects, i.e., those arising from terms in the Hamiltonian having quadratic dependence on spin components.

The $\epsilon_i^{\mu,j}$ are the irreducible strains with the symmetry of the hexagonal close-packed structure.[17] They are related to the usual strains defined with respect to Cartesian axes in the following manner:

$$\begin{aligned}
\epsilon^{\alpha,1}&=\epsilon_{\xi\xi}+\epsilon_{\eta\eta}+\epsilon_{\zeta\zeta},\\
\epsilon^{\alpha,2}&=\tfrac{1}{3}(2\epsilon_{\zeta\zeta}-\epsilon_{\xi\xi}-\epsilon_{\eta\eta}),\\
\epsilon_1^{\gamma}&=\tfrac{1}{2}(\epsilon_{\xi\xi}-\epsilon_{\eta\eta}),\\
\epsilon_2^{\gamma}&=\epsilon_{\xi\eta},\\
\epsilon_1^{\epsilon}&=\epsilon_{\eta\zeta},\\
\epsilon_2^{\epsilon}&=\epsilon_{\zeta\xi},
\end{aligned} \tag{3.6}$$

where the Cartesian strains are defined as usual:

$$\epsilon_{ij}=\tfrac{1}{2}[(\partial\rho_i/\partial r_j)+(\partial\rho_j/\partial r_i)], \qquad (i,j=\xi,\eta,\zeta) \tag{3.7}$$

with ρ as the displacement of a point relative to its equilibrium position. The c_{jh}^{μ} are the elastic stiffness constants which are related to the five independent Cartesian stiffness constants by the relations

$$\begin{aligned}
c_1^{\alpha}&=\tfrac{1}{9}(2c_{11}+2c_{12}+4c_{13}+c_{33}),\\
c_2^{\alpha}&=\tfrac{1}{2}(c_{11}+c_{12}-4c_{13}+2c_{33}),\\
c_{12}^{\alpha}&=\tfrac{1}{3}(-c_{11}-c_{12}+c_{13}+c_{33}),\\
c^{\gamma}&=2(c_{11}-c_{12}),\\
c^{\epsilon}&=4c_{44}.
\end{aligned} \tag{3.8}$$

[17] E. Callen and H. B. Callen, Phys. Rev. **139**, A455 (1965).

The constants $B_n^{\mu,l}$ give the phenomenological magnetoelastic constants up to second order in the direction cosines, α_i, of the magnetization relative to the crystallographic axis. The $B_n^{\mu,l}$ have temperature dependence proportional to that of the square of component of moment along the equilibrium magnetization direction.

The equilibrium values of the strains arising from a given net magnetization are determined by minimizing the total strain-dependent energy density, $E_{MS}=E_E+E_M$, with respect to each of the strain components. To consider the spiral to ferromagnetic transition in Dy, we are interested in the strains developed for magnetization in the plane, i.e., $\alpha_\zeta=0$. Then we need consider only ϵ_1^{γ} and ϵ_2^{γ}. The equilibrium values of these strains are

$$\begin{aligned}
\bar{\epsilon}_1^{\gamma}&=(1/2c^{\gamma})(\alpha_\xi^2-\alpha_\eta^2)B^{\gamma,2},\\
\bar{\epsilon}_2^{\gamma}&=(1/c^{\gamma})\alpha_\xi\alpha_\eta B^{\gamma,2}.
\end{aligned} \tag{3.9}$$

Then the total strain-dependent energy density for a given net magnetization is found by substituting these expressions into (3.4) and (3.5). In particular, for Dy with magnetization along an easy ξ axis,

$$\bar{E}_{MS}=-\tfrac{1}{2}c^{\gamma}(\bar{\epsilon}_1^{\gamma})^2. \tag{3.10}$$

The saturation magnetostriction $\lambda=\delta l/l$ is given by

$$\begin{aligned}
\lambda=\delta l/l=&\tfrac{1}{3}\lambda_{11}^{\alpha}(T)+(\tfrac{1}{2}\sqrt{3})\lambda_{12}^{\alpha}(T)(\alpha_\zeta^2-\tfrac{1}{3})\\
&+2\lambda_{21}^{\alpha}(T)(\beta_\zeta^2-\tfrac{1}{3})+\sqrt{3}\lambda_{22}^{\alpha}(T)(\alpha_\zeta^2-\tfrac{1}{3})(\beta_\zeta^2-\tfrac{1}{3})\\
&+2\lambda^{\gamma}(T)\{\tfrac{1}{4}(\alpha_\xi^2-\alpha_\eta^2)(\beta_\xi^2-\beta_\eta^2)+\alpha_\xi\alpha_\eta\beta_\xi\beta_\eta\}\\
&+2\lambda^{\epsilon}(T)\{\alpha_\eta\alpha_\zeta\beta_\eta\beta_\zeta+\alpha_\xi\alpha_\zeta\beta_\xi\beta_\zeta\},
\end{aligned} \tag{3.11}$$

where the β_i are the direction cosines relative to the crystal axes of the direction of observation. (Here in particular, the coefficient λ^{γ} represents the distortion of the circular symmetry of the basal plane by the rotation of the component of the magnetization in the plane.)

The equilibrium strains are given by

$$\begin{aligned}
\bar{\epsilon}_1^{\gamma}&=\lambda^{\gamma}\tfrac{1}{2}(\alpha_\xi^2-\alpha_\eta^2),\\
\bar{\epsilon}_2^{\gamma}&=\lambda^{\gamma}\alpha_\xi\alpha_\eta,
\end{aligned} \tag{3.12}$$

so that the equilibrium energy of magnetostriction is given by

$$\bar{E}_{MS}=-\tfrac{1}{8}c^{\gamma}(\lambda^{\gamma})^2. \tag{3.13}$$

This is the term in the free energy that provides the driving force for the spiral to ferromagnetic transition at the Curie temperature in Dy and Tb, and that aids an applied field in driving this transition at temperatures above T_c. We evaluated $\bar{E}_{MS}$ in Ref. 3 by assuming c^{γ} to be temperature-independent and the tem-

perature dependence of λ^γ to be given by the theory of Callen and Callen[17]:

$$\lambda^\gamma=\lambda(0)\hat{I}_{5/2}[\mathcal{L}^{-1}(\sigma)]. \tag{3.14}$$

Then, using experimental values for $\lambda(0)$ and c^γ, we found $\tilde{E}_{\rm MS}$ to be closely equal to the experimental value for the spiral to ferromagnet driving energy for a considerable range of temperature above T_c. (There is a second, much smaller contribution to the driving energy, the hexagonal planar anisotropy energy of the undistorted lattice.)

4. MAGNETOELASTIC EFFECTS ON THE SPIN-WAVE BEHAVIOR: FROZEN-LATTICE APPROXIMATION

Turov and Shavrov[4] have suggested a very provocative idea for the magnetoelastic effects on the spin-wave energy gap at $\mathbf{q}=0$ for the ferromagnetically aligned heavy rare-earth metals. Basically, their idea is as follows: The lowest-order terms in the free energy giving rise to the equilibrium magnetostriction have cylindrical symmetry about the c axis. (These are the terms discussed in Sec. 3 above.) Thus, for any direction of magnetization in the hexagonal plane, the strain arising from magnetostriction at some specified angle relative to the magnetization will be the same. Turov and Shavrov suggest that the correct way to find the uniform-mode frequency is to regard the strain as frozen at its equilibrium position. Then in the excited state, the relative orientation of moment and strain changes, and there is a net increase of energy relative to the equilibrium state associated with magnetostriction effects *even though the equilibrium energy associated with the magnetostriction has cylindrical symmetry*. Using the macroscopic equation of motion technique and approximate values for the relevant experimental parameters, they estimated this effect as giving an energy gap of about 10°K for the $\mathbf{q}=0$ mode in dysprosium. Thus, the effects they suggest are quite significant.

In the present section we will give these ideas more detailed treatment than is contained in the paper by Turov and Shavrov. To do this, we consider the magnetostriction effects on the long-wavelength spin waves using the same sort of effective spin Hamiltonian used by Callen and Callen[17] to treat the equilibrium magnetostriction. In this treatment the strains are treated as classical quantities. This is consistent with the fact that the strains considered correspond to the homogeneous strain modes for which the natural vibrational frequencies vanish.

Then the relevant equilibrium strains to be considered are those affected by motion of the spins in the hexagonal plane, $\bar{\epsilon}_1^\gamma$ and $\bar{\epsilon}_2^\gamma$. [The other strain terms will give effective fields entering into the same factor in the expression for $\omega(0)$ as the large axial anisotropy field. Any effect caused by them will be negligible as compared with the large axial anisotropy field.] In the frozen-lattice approximation this then gives the following spin Hamiltonian to be used in determining the long-wavelength spin-wave frequencies:

$$\begin{aligned}\mathcal{H}=&-\sum_{i\neq j}J_{ij}\mathbf{S}_i\cdot\mathbf{S}_j-P_2\sum_i S_{i\zeta}{}^2+\tfrac{1}{2}P_6{}^6\sum_i[(S_{i\xi}+iS_{i\eta})^6\\&+(S_{i\xi}-iS_{i\eta})^6]-g\beta H_{||}\sum_i S_{i\xi}-g\beta H_\perp\sum_i S_{i\eta}\\&-\tilde{B}^\gamma[\tfrac{1}{2}\bar{\epsilon}_1{}^\gamma\sum_i(S_{i\xi}{}^2-S_{i\eta}{}^2)+\bar{\epsilon}_2{}^\gamma\sum_i(S_{i\xi}S_{i\eta})].\end{aligned} \tag{4.1}$$

Here, as in Sec. 2, we take ξ as the easy planar axis. Then $H_{||}$ is the component of field along ξ, and $H_\perp$ is that perpendicular to ξ. $\tilde{B}^\gamma$ is the magnetoelastic coupling constant,[17] and is determined using the experimental value of the saturation magnetostriction coefficient, λ^γ, and the elastic constant c^γ. The equilibrium strains $\bar{\epsilon}_1{}^\gamma$ and $\bar{\epsilon}_2{}^\gamma$ are also obtained from the experimental values of λ^γ.

To find the spin-wave dispersion law for the Hamiltonian of (4.1) involves using the transformation given in (2.13) so that the z axis is taken along the equilibrium magnetization direction. Then keeping the quadratic terms gives

$$\begin{aligned}\mathcal{H}=&-\sum_{i\neq j}J_{ij}(S_i{}^+S_j{}^-+S_{iz}S_{jz})-P_2\sum_i S_{ix}{}^2+P_6{}^6\sum_i\\&\times(S_{iz}{}^6\cos6\delta-15S_{iz}{}^4S_{iy}{}^2\cos6\delta)-g\beta H_{||}\cos\delta\sum_i S_{iz}\\&-g\beta H_\perp\sin\delta\sum_i S_{iz}+\tfrac{1}{4}(\tilde{B}^\gamma\lambda^\gamma)\sum_i(S_{iy}{}^2-S_{iz}{}^2).\end{aligned} \tag{4.2}$$

Here we have used the relationship between the equilibrium strains and the experimentally measured magnetostriction coefficient λ^γ:

$$\bar{\epsilon}_1{}^\gamma=\tfrac{1}{2}\lambda^\gamma\cos2\delta, \tag{4.3a}$$

$$\bar{\epsilon}_2{}^\gamma=\tfrac{1}{2}\lambda^\gamma\sin2\delta, \tag{4.3b}$$

where δ is determined by (2.15) and (2.16).

Then the diagonalization of $\mathcal{H}$ using spin-wave boson operators proceeds in the usual way to give (at $T=0$)

$$\begin{aligned}\hbar\omega(\mathbf{q})=\{&[2SJ(0)-2SJ(\mathbf{q})-2P_2S-6P_6{}^6S^5\cos6\delta\\&+g\beta H_{||}\cos\delta+g\beta H_\perp\sin\delta+\tfrac{1}{2}(\tilde{B}^\gamma\lambda^\gamma S)][2SJ(0)\\&-2SJ(\mathbf{q})-36P_6{}^6S^5\cos6\delta+g\beta H_{||}\cos\delta\\&+g\beta H_\perp\sin\delta+\tilde{B}^\gamma\lambda^\gamma S]\}^{1/2}.\end{aligned} \tag{4.4}$$

To treat the temperature dependence of $\hbar\omega(\mathbf{q})$, we express the magnetoelastic coupling constant in terms of λ^γ and c^γ, the experimentally determined elastic constant:

$$\tilde{B}^\gamma=3c^\gamma\lambda^\gamma/S(2S-1). \tag{4.5}$$

Then defining the quantity D^γ by the relationship

$$2D^\gamma\equiv\tilde{B}^\gamma(T=0)\lambda^\gamma(T=0)\,S=\frac{3c^\gamma(T=0)\,(\lambda^\gamma[T=0])^2}{(2S-1)}, \tag{4.6}$$

Equation (4.4) becomes for $T=0$

$$\hbar\omega(\mathbf{q})=\{[2SJ(0)-2SJ(\mathbf{q})-2P_2S-6P_6{}^6S^5\cos6\delta+g\beta H_{||}\cos\delta+g\beta H_\perp\sin\delta+D^\gamma][2SJ(0)-2SJ(\mathbf{q})-36P_6{}^6S^5\cos6\delta+g\beta H_{||}\cos\delta+g\beta H_\perp\sin\delta+2D^\gamma]\}^{1/2}. \tag{4.7}$$

To find the temperature dependence, we use the result of Callen and Callen[17] that $\lambda^\gamma\sim\hat{I}_{5/2}[\mathfrak{L}^{-1}(\sigma)]$. This has been confirmed experimentally for Dy by Clark *et al.*[18] and for Tb by Rhyne and Legvold.[19] The temperature dependence of c^γ is expected to be small. (For Er, where data[20] is available below room temperature, c^γ decreases slightly less than 8% between 63 and 298°K.) Then the temperature dependence of the D^γ term is proportional to $(1/\sigma)(\hat{I}_{5/2})^2$.

For H along an easy axis, including the T dependence, (4.7) becomes

$$\hbar\omega(\mathbf{q})=\{(2S\sigma[J(0)-J(\mathbf{q})]-2P_2S(\hat{I}_{5/2}/\sigma)-6P_6{}^6S^5(\hat{I}_{13/2}/\sigma)+g\beta H+(D^\gamma[\hat{I}_{5/2}]^2/\sigma))(2S\sigma[J(0)-J(\mathbf{q})]-36P_6{}^6S^5(\hat{I}_{13/2}/\sigma)+g\beta H+2D^\gamma([\hat{I}_{5/2}]^2/\sigma))\}^{1/2}. \tag{4.8}$$

For H along a hard axis, (4.7) becomes

$$\hbar\omega(\mathbf{q})=\{(2S\sigma[J(0)-J(\mathbf{q})]-2P_2S(\hat{I}_{5/2}/\sigma)-6P_6{}^6S^5\cos6\delta(\hat{I}_{13/2}/\sigma)+g\beta H\cos(\tfrac{1}{6}\pi-\delta)+(D^\gamma[\hat{I}_{5/2}]^2/\sigma))(2S\sigma[J(0)-J(\mathbf{q})]-36P_6{}^6S^5\cos6\delta\times(\hat{I}_{13/2}/\sigma)+g\beta H\cos(\tfrac{1}{6}\pi-\delta)+(2D^\gamma[\hat{I}_{5/2}]^2/\sigma))\}^{1/2}, \tag{4.9}$$

where δ is determined from (2.15) and (2.16).

We have the result then that (4.8) and (4.9) give the magnetoelastic effect on spin-wave energies based on the frozen-lattice assumption, i.e., that for long-wavelength excitations the strain due to magnetostriction stays frozen in its equilibrium position. We will discuss the relevance of this result to experiment in Sec. 7. Before doing so, in the next section we consider the other possible physical extreme. This is that the uniform strain associated with magnetostriction is able to follow the nearly-uniform motion of the magnetization in the long-wavelength modes. In that case, the magnetoelastic, D^γ, contribution to the spin-wave energies, given in (4.8) and (4.9), and associated with the lowest-order magnetostriction effects (that giving rise to an equilibrium energy having cylindrical symmetry) vanishes.

Physically, this is quite obvious. Roughly speaking, the two factors within the square root in the expressions for $\hbar\omega(\mathbf{q})$ in (4.8) or (4.9) represent two different effective fields governing the motion of the magnetic moment on departure from equilibrium. The first factor gives the effective field perpendicular to the equilibrium-moment direction. In this factor, typically the axial anisotropy, P_2, term is dominant and the magnetoelastic, D^γ, term and the planar anisotropy, $P_6{}^6$, term have little effect. On the other hand, the second factor gives the effective field parallel to the equilibrium-moment direction; and this effect, for long wavelengths, is completely given by the magnetoelastic and planar anisotropy effects, together with that of applied field in the plane. Clearly, if the strain is free to follow the motion of the moment, and if the energy associated with magnetostriction has cylindrical symmetry, then the magnetoelastic contribution to the spin-wave energies vanishes. In this case, there can still be a magnetoelastic contribution to the spin-wave energies, but it corresponds to higher-order magnetostriction effects, those giving an equilibrium energy with hexagonal rather than cylindrical symmetry. Experimentally, for Tb, the measurements of Rhyne and Legvold[19] separated out the higher-order magnetostriction effects having hexagonal symmetry from the lowest-order, cylindrically symmetric, effects.

5. MAGNETOELASTIC EFFECT ON SPIN-WAVE ENERGIES WHEN FROZEN-LATTICE APPROXIMATION DOES NOT APPLY

We now consider the contribution of the second-order, hexagonally symmetric, magnetostriction terms to the long-wavelength spin-wave energies in the event that the frozen-lattice approximation does not apply. Mason[21] has discussed in considerable detail the symmetry restrictions placed on the form of the elastic and magnetoelastic contributions to the free energy in a hexagonal material. Following that treatment, the contributions to the elastic and magnetoelastic energies related to change in direction of magnetic moment within the hexagonal plane are given by

$$E_{\mathrm{E}}=\tfrac{1}{2}c^\gamma[(\epsilon_1{}^\gamma)^2+(\epsilon_2{}^\gamma)^2], \tag{5.1}$$

$$E_{\mathrm{M}}=\epsilon_1{}^\gamma[2C_1(\alpha_\xi{}^2-\alpha_\eta{}^2)-C_2+8C_2\alpha_\xi{}^2\alpha_\eta{}^2]+\epsilon_2{}^\gamma[4C_1\alpha_\xi\alpha_\eta+4C_2\alpha_\xi\alpha_\eta(\alpha_\xi{}^2-\alpha_\eta{}^2)]. \tag{5.2}$$

Here α_ξ and α_η are the directional cosines of the magnetization with respect to the ξ and η axes, respectively. The constants C_1 and C_2 then give the magnitude of the first- and second-order magnetoelastic energies. The equilibrium strains are then found by minimizing the total energy associated with magnetostriction,

$$E_{\mathrm{MS}}=E_{\mathrm{E}}+E_{\mathrm{M}}, \tag{5.3}$$

with respect to strain. This yields

$$\bar{\epsilon}_1{}^\gamma=-(1/c^\gamma)[2C_1(\alpha_\xi{}^2-\alpha_\eta{}^2)+8C_2\alpha_\xi{}^2\alpha_\eta{}^2-C_2], \tag{5.4a}$$

$$\bar{\epsilon}_2{}^\gamma=-(1/c^\gamma)[4C_1\alpha_\xi\alpha_\eta+4C_2\alpha_\xi\alpha_\eta(\alpha_\xi{}^2-\alpha_\eta{}^2)]. \tag{5.4b}$$

[18] A. E. Clark, B. F. DeSavage, and R. Bozorth, Phys. Rev. **138**, A216 (1965).
[19] J. J. Rhyne and S. Legvold, Phys. Rev. **138**, A507 (1965).
[20] E. S. Fisher and D. Dever, Trans. Met. Soc. AIME **239**, 48 (1967).
[21] W. P. Mason, Phys. Rev. **96**, 302 (1954).

Then by comparison with the corresponding expressions of Rhyne and Legvold,[19] we obtain the relationship between the parameters C_1 and C_2 and the experimentally measured first- and second-order magnetostriction coefficients, $C(\equiv\frac{1}{2}\lambda^\gamma)$ and A in the notation of Rhyne and Legvold:

$$C_1=-\tfrac{1}{2}c^\gamma C=-\tfrac{1}{4}(c^\gamma\lambda^\gamma), \tag{5.5a}$$

$$C_2=-\tfrac{1}{2}(c^\gamma A). \tag{5.5b}$$

Substituting the equilibrium strains given in (5.4a) into (5.3) gives the equilibrium energy associated with the first- and second-order magnetostriction effects:

$$\bar{E}_{\rm MS}=\bar{E}_{\rm cyl}+\bar{E}_{\rm hex}. \tag{5.6}$$

Here

$$\bar{E}_{\rm cyl}=-\tfrac{1}{8}[c^\gamma(\lambda^\gamma)^2](\alpha_\xi^2+\alpha_\eta^2)^2 \tag{5.7}$$

is the lowest-order energy, already discussed in Sec. 3, and has cylindrical symmetry. On the other hand, the energy $\bar{E}_{\rm hex}$ associated with the second-order magnetostriction effects has hexagonal symmetry:

$$\bar{E}_{\rm hex}=\tfrac{1}{4}(c^\gamma\lambda^\gamma A)\cos 6\phi. \tag{5.8}$$

Experimentally,[19] the parameters C(or λ^γ) and A, distinguishing the first- and second-order magnetostriction effects, are obtained using the expression for the a axis magnetostriction accompanying a rotation of the magnetostriction through an angle ϕ in the basal plane

$$\delta l/l=-2C\sin^2\phi+A\sin^2 2\phi. \tag{5.9}$$

Since $\bar{E}_{\rm hex}$, given in (5.8) has hexagonal symmetry, there is a corresponding magnetostriction contribution to the uniform-mode energy, even when the frozen-lattice approximation does not apply, and the strain assumes an instantaneous equilibrium value following the motion of the magnetization. By comparison with (2.6), the value of $\hbar\omega(0)$ is obtained by the replacement

$$K_6(T)=L_6(T)+\tfrac{1}{4}(c^\gamma\lambda^\gamma A), \tag{5.10}$$

where $L_6(T)$ represents that part of the planar anisotropy constant given by the single-ion crystal-field effects for the unstrained lattice. Then

$$\hbar\omega(0)=(g\beta/M)\{[2K_2(T)+6(L_6(T)+\tfrac{1}{4}(c^\gamma\lambda^\gamma A))] \times[36(L_6(T)+\tfrac{1}{4}(c^\gamma\lambda^\gamma A))]\}^{1/2}. \tag{5.11}$$

According to the theory of Callen and Callen,[17] the temperature dependence of A goes as $\hat{I}_{9/2}[\mathcal{L}^{-1}(\sigma)]$. This is borne out for Tb by the measurements of Rhyne and Legvold.[19] Therefore, the temperature-dependent expression for the uniform-mode frequency including the energy associated with the magnetostriction terms of hexagonal symmetry is

$$\hbar\omega(0)=(g\beta/M)\{[2K_2(0)\hat{I}_{5/2}+6(L_6(0)\hat{I}_{13/2} +\tfrac{1}{4}[c^\gamma\lambda^\gamma(0)A(0)]\hat{I}_{5/2}\hat{I}_{9/2})][36(L_6(0)\hat{I}_{13/2} +\tfrac{1}{4}[c^\gamma\lambda(0)A(0)]\hat{I}_{5/2}\hat{I}_{9/2})]\}^{1/2}. \tag{5.12}$$

6. VALUES OF PARAMETERS

Before discussing the relevance of the preceding theory to the neutron-scattering and magnetic-resonance experiments, it is necessary to obtain values for the various parameters entering the theory. We first discuss the values for the elastic constant c^γ. For Dy, the value at 298°K is directly obtained from the measurements of Fisher and Dever[20] using the definition given in (3.8):

$$\text{Dy},\ c^\gamma=0.97\times10^{12}\ \text{erg/cm}^3=22.2\times10^4\ ^\circ\text{K/atom}. \tag{6.1}$$

For Tb, there are no direct measurements of the relevant elastic constants available. However, one can extrapolate[11] from Dy using measurements by Smith *et al.*[22] of the longitudinal and shear elastic-wave velocities for polycrystalline Dy and Tb. This involves the assumption that the elastic constant varies as the product of the density and the square of the elastic-wave velocity.

$$c^\gamma\sim\rho v^2_{\rm elas}. \tag{6.2}$$

This then would give a value of c^γ for Tb equal to 0.94 that of Dy (using the longitudinal velocity) or 0.895 that of Dy (using the shear velocity). Taking the average of these two possibilities gives

$$\text{Tb},\ c^\gamma=0.89\times10^{12}\ \text{erg/cm}^3=20.33\times10^4\ ^\circ\text{K/atom}. \tag{6.3}$$

The extrapolation scheme can be checked by extrapolating from Dy to Er, for which experimental results are also available. Doing this gives c^γ within 5% of the experimental value for Er.

This value of c^γ can be combined with the value of λ^γ at $T=0$ to obtain the parameter D^γ defined by (4.6) which gives the magnetoelastic effect on the spin-wave energies in the frozen-lattice approximation. For[18] Dy,

$$\text{Dy}\quad\lambda^\gamma(T=0)=8.5\times10^{-3}, \tag{6.4}$$

which gives

$$\text{Dy}\quad 2D^\gamma=3.43^\circ\text{K/atom}. \tag{6.5}$$

This compares with a value for $36P_6{}^6S^5$ obtained from the anisotropy-constant measurements of Liu *et al.*[9,23] on the basis that the planar hexagonal anisotropy constant is completely due to crystal-field effects of the unstrained lattice:

$$\text{Dy}\quad 36\,P_6{}^6S^5=-11.5^\circ\text{K/atom}. \tag{6.6}$$

For Tb, λ^γ is obtained from the measurements of Rhyne and Legvold,[19]

$$\text{Tb}\quad\lambda^\gamma(T=0)=8.8\times10^{-3}. \tag{6.7}$$

This gives

$$\text{Tb}\quad 2D^\gamma=4.35^\circ\text{K/atom}. \tag{6.8}$$

---

[22] J. F. Smith, C. E. Carlson, and F. H. Spedding, J. Metals **9**, 1212 (1957).

[23] The measurements of Rhyne and Clark (Ref. 5) give $36P_6{}^6S^5=-8.33^\circ$K/atom for Dy.

Again this can be compared with $36P_6{}^6S^5$ obtained from the anisotropy-constant measurements of Rhyne and Clark,[5] if one assumes that the planar anisotropy constant is completely due to crystal-field effects of the unstrained crystal:

$$\text{Tb} \quad 36\,P_6{}^6S^5 = -3.4^\circ\text{K/atom}. \qquad (6.9)$$

Thus, examining (4.8) and (4.9) we expect that for both Dy and, especially, Tb the magnetoelastic contribution to the long-wavelength spin-wave energies associated with the lowest-order, cylindrically symmetric, magnetostriction effects will be quite significant if the frozen-lattice approximation holds. (Actually, for Tb, as discussed immediately below, a large part of the macroscopic planar anisotropy constant is probably due to the second-order, hexagonally symmetric magnetostriction effects. However, this does not effect our statement about the importance of the effects associated with lowest-order magnetostriction in the frozen-lattice approximation.)

We can also consider the relevant magnitudes if the frozen-lattice approximation does not hold, and the magnetoelastic contribution to $\hbar\omega(0)$ is given by (5.12). Since the lowest-order, cylindrically symmetric and higher-order, hexagonally symmetric, magnetostriction effects have been experimentally separated for Tb but not for Dy, this is possible only for Tb.

Then, at $T=0$ from Rhyne and Clark's[5] measurement for Tb,

$$\text{Tb} \quad K_6 = 2.4\times10^6 \text{ erg/cm}^3; \qquad (6.10)$$

while using the experimental values of Rhyne and Legvold,[19]

$$\text{Tb} \quad c^\gamma\lambda^\gamma A/4 = 4.14\times10^6 \text{ erg/cm}^3. \qquad (6.11)$$

The measurements and analysis of Rhyne and Clark[5] are such that their value of K_6 should include both the hexagonal anisotropy of the unstrained crystal and that associated with magnetostriction as given by (5.10). This then indicates that the magnitude of the contribution of the magnetostriction-associated hexagonal anisotropy is comparable to the total hexagonal anisotropy constant. Indeed, the present estimate of the strain-dependent anisotropy in (6.11) actually exceeds the total measured hexagonal anisotropy constant in (6.10). This excess would indicate that the hexagonal crystal field for the unstrained lattice favors alignment along the a (hard) axis for Tb. However, the numerical values in (6.10) and (6.11) probably contain substantial uncertainty. For example, in Dy the value found by Liu *et al.*[9] for K_6 by analysis of the magnetization behavior exceeds that found by Rhyne and Clark[5] by analysis of magnetostriction data by about 40%. Probably the strongest statement that can be safely made is that the hexagonal anisotropy associated with strains due to magnetoelastic effects gives a large, and probably dominant, contribution to the total hexagonal planar anisotropy constant.

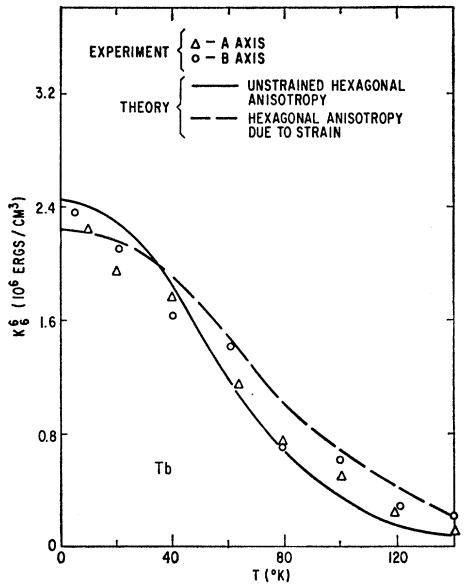

FIG. 2. Basal-plane anisotropy of terbium obtained from magnetostriction data compared with theory. Results from both a and b axis strain measurements are shown. [Solid curve and experimental points are from J. J. Rhyne and A. E. Clark, J. Appl. Phys. **38**, 1379 (1967)].

In practice the difference in behavior between a hexagonal anisotropy caused by the crystal field of the unstrained lattice [$L_6(T)$ of (5.10)] and that caused by strain [$\frac{1}{4}(c^\gamma\lambda^\gamma A)$ of (5.10)] is not very great. The temperature dependence of the former goes as $\hat{I}_{13/2}[\mathcal{L}^{-1}(\sigma)]$; while that of the latter goes as $\hat{I}_{5/2}[\mathcal{L}^{-1}(\sigma)]\hat{I}_{9/2}[\mathcal{L}^{-1}(\sigma)]$. In Fig. 2 we show the comparison of both of these types of temperature dependence to the experimental values for K_6, where the $\hat{I}_{5/2}\hat{I}_{9/2}$ dependence matched at low T has been superimposed on Fig. 2 of Rhyne and Clark,[5] which already contained the curve with $\hat{I}_{13/2}$ dependence. (The magnetization data of Hegland *et al.*[24] has been used in the calculations throughout this paper involving the reduced magnetization of Tb.) On the basis of the experimental data, there is no very strong case for choosing one of the theoretical curves over the other.

7. DISCUSSION OF EXPERIMENTAL RESULTS FOR $\hbar\omega(0)$ IN Tb AND Dy

In this section we discuss the application of the theoretical results of the preceding sections to understanding the observed long-wavelength spin-wave behavior for Tb and Dy. (In all calculations involving the reduced magnetization, we use the magnetization data of Hegland *et al.*[24] for Tb and of Behrendt *et al.*[25] for Dy.) In particular, we discuss the relevance of the frozen-lattice approximation to the observed behavior.

[24] D. E. Hegland, S. Legvold, and F. H. Spedding, Phys. Rev. **131**, 158 (1963).
[25] D. R. Behrendt, S. Legvold, and F. H. Spedding, Phys. Rev. **109**, 1544 (1958).

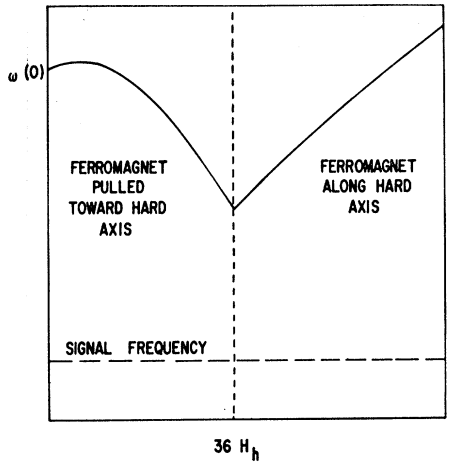

FIG. 3. Field variation of $\omega(0)$ for ferromagnet with H along a hard planar axis, including magnetoelastic effects in the frozen-lattice approximation.

In this connection there are two key qualitative points to make about the $\mathbf{q}=0$ spin-wave behavior to be expected when the frozen-lattice approximation is applicable. The energy for the $\mathbf{q}=0$ mode, given by (4.8) or (4.9), essentially corresponds to the geometric mean of two effective fields, one perpendicular to the equilibrium direction of magnetization and one parallel to that direction. These correspond respectively to the first and second factors on the right-hand side of (4.8) or (4.9). The D^γ term in the second factor, coming from the lowest-order magnetostriction effects in the frozen-lattice approximation, falls off much more slowly with increasing temperature than the other contributions to the second factor. Thus, for relative values of parameters as given in Sec. 6, the D^γ term dominates the effective field parallel to the direction of magnetization for increasing temperature. This causes the long-wavelength spin-wave energy to decrease much more slowly with temperature when the frozen-lattice effect applies than otherwise.

The second key point refers to an even more striking qualitative difference predicted for the frozen-lattice case as compared with other possibilities. This is the fact pointed out by Turov and Shavrov,[4] that the contribution of magnetostriction effects to the value of $\hbar\omega(0)$, the spin-wave gap, because it comes from an energy of cylindrical symmetry, is isotropic. Thus, typical behavior for $\hbar\omega(0)$ with H applied along a hard planar axis gives behavior as shown in Fig. 3. In contrast to the behavior illustrated in Fig. 1 for vanishing magnetoelastic effects, $\hbar\omega(0)$ does not go to zero at $36H_h$. Thus, a field applied along the hard planar axis can be used to separate out any contribution to $\hbar\omega(0)$ of the frozen-strain type.

In Ref. 3, we have noted that the temperature dependence of the $\mathbf{q}=0$ spin-wave energy for Tb found in neutron inelastic scattering experiments precludes the applicability of the frozen-lattice approximation. This is demonstrated by the results shown in Fig. 4.

The experimental values for $\hbar\omega(0)$ shown in Fig. 4 involve extrapolating the measured dispersion curve[7,7a] to $\mathbf{q}=0$. (The smallest $\mathbf{q}$ actually measured is about 10% of the distance to the zone boundary.)

In addition to the experimental points, three theoretical curves are also shown in Fig. 4. For all three calculations, P_2 has been taken as the experimental value.[5]

$$\text{Tb}, \quad P_2S=-31.8°\text{K/atom}. \tag{7.1}$$

The three curves have been matched at 90°K to the experimental value of $\hbar\omega(0)$ found by neutron inelastic scattering.[6,7,7a]

The short-dashed curve labeled "Frozen-Lattice Approximation" was obtained using (4.8) by taking P_6^6 as the value given in (6.9) and taking D^γ to give the neutron $\hbar\omega(0)$ at 90°K. This requires $2D^\gamma=2.98°\text{K/atom}$, which is only about 70% of the value given in (6.8) found from equilibrium measurements.

The solid curve was obtained by putting D^γ in (4.8) equal to zero and taking a value of P_6^6 necessary to match the experimental $\hbar\omega(0)$ at 90°K. This requires $36P_6^6S^5=-12.55°\text{K/atom}$. This value is 3.7 times that given in (6.9) (which is the value obtained from the macroscopic planar anisotropy constant if one assumes that the planar anisotropy constant is completely due to crystal-field effects of the unstrained crystal). A similar discrepancy has been noted by Møller *et al.*[6] [Møller *et al.* quote values for their parameters B and G at 110°K for a Tb–10% Ho alloy that correspond to the following values of parameters at $T=0$: $P_2S=-22.06°\text{K/atom}$ and $36P_6^6S^5=-18.2°\text{K/atom}$. Their values for the two parameters are different from ours because they have obtained their value for P_2 from the neutron group intensities at 110°K, and this value is about 30% lower than our value in (7.1) obtained from torque measurements. However, their P_6^6 is correspondingly greater than ours so that the product of

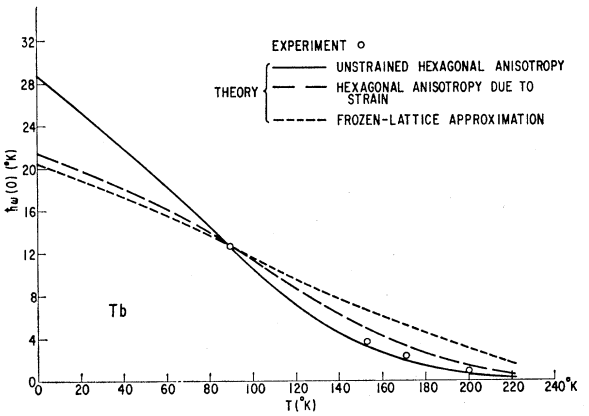

FIG. 4. Temperature dependence of $\mathbf{q}=0$ spin-wave energy for Tb.

P_2 and P_6^6 giving $\hbar\omega(0)$ at $T=0$ is the same as ours within less than 1%.] The solid curve then gives the "ordinary" result with no magnetostriction, that is, the effective fields giving the $\mathbf{q}=0$ spin-wave energy come from the axial and planar crystal-field anisotropy of the unstrained crystal.

The third, long-dashed, curve puts D^γ in (4.8) equal to zero, and replaces the $P_6^6\hat{I}_{13/2}$ term by one going as $\hat{I}_{5/2}\hat{I}_{9/2}$. This represents the case where the hexagonal anisotropy is caused by magnetoelastic effects. For this case, one of course, has exactly the same discrepancy already noted for the "ordinary" case (where the hexagonal anisotropy is caused by the crystal field of the unstrained crystal) between the experimental magnitude of the macroscopic planar anisotropy constant and the magnitude required to explain the experimental value of $\hbar\omega(0)$ at 90°K. While there is substantial scatter in the experimental values of the macroscopic planar anisotropy constant K_6^6 shown in Fig. 2, the value of K_6^6 at 90°K would have to be almost four times larger than the value given by the solid curve in Fig. 2 to remove this discrepancy.

On the other hand, if we put aside the question of a discrepancy between the static measurement of planar anisotropy and that required to match experiment at 90°K, we can compare the three theoretical curves to the experimental values of $\hbar\omega(0)$ at higher temperatures. The experimental spin-wave energies fall between the two curves for which the strain is not frozen. This argues against the applicability of the frozen-lattice approximation. Actually, there are other experimental results arguing much more forcefully against the applicability of the frozen-lattice approximation for the magnetoelastic behavior for understanding the behavior of the energy for long-wavelength spin waves in Tb and Dy. These are the observations of ferromagnetic resonance[8,10,11] in Tb and Dy at 9.44 GHz and 37.7 GHz, respectively.

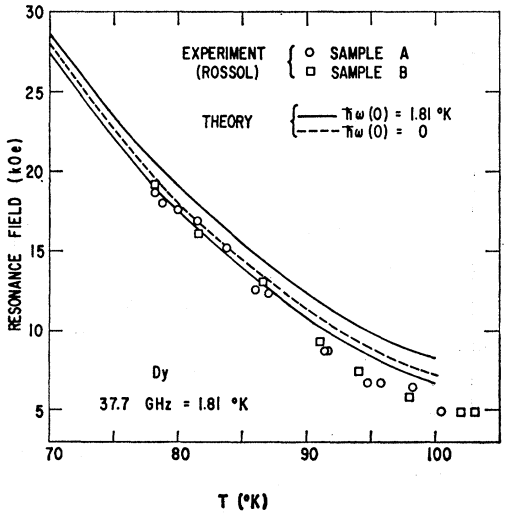

FIG. 5. Temperature dependence of resonance field in Dy at 37.7 GHz for H along a hard axis in the basal plane.

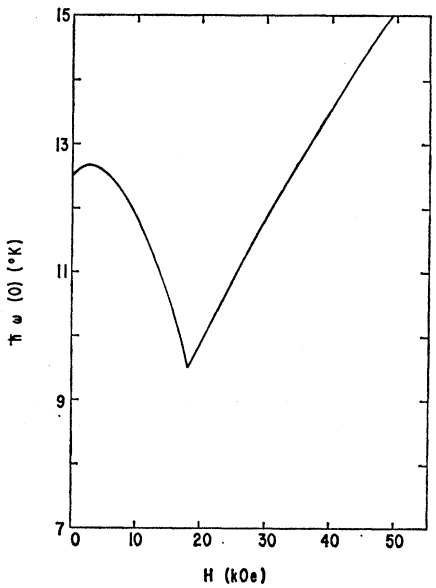

FIG. 6. Theoretical field dependence of $\mathbf{q}=0$ spin-wave energy for Dy at 80°K with H along a hard axis in the basal plane, when magnetoelastic effects are included using the frozen-lattice approximation.

When the frozen-lattice approximation is inapplicable, as illustrated in Fig. 1, a magnetic field applied along a hard hexagonal axis can reduce $\omega(0)$ to zero. When $\omega(0)$ matches the signal frequency, one can observe resonant absorption. On the other hand, because of the cylindrical symmetry of the lowest-order magnetostriction energy, as pointed out by Turov and Shavrov,[4] one cannot drive $\omega(0)$ to zero with an applied field along a hard planar axis. For example, at 90°K our calculations for the frozen-lattice case in Tb predict that $\hbar\omega(0)$ cannot be reduced below 10.8°K. (This occurs for 8 kOe along a hard axis.) Thus, for the frozen-lattice case, Fig. 3 illustrates a typical situation. The minimum value of $\omega(0)$ falls well above the signal frequency, and one expects no resonant absorption. We will now discuss the resonance experiments in Dy and Tb in more detail.

The experimental values of resonant field applied along a hard planar axis found by Rossol and Jones[10,11] for Dy at 37.7 GHz are shown in Fig. 5. For temperatures above 85°K, the magnetic arrangement in zero applied field is actually a spiral. However, for the lower-temperature part of the spiral regime in which these observations occur, the planar anisotropy effects are still quite important. Then the situation is basically the same as that shown in Fig. 1, except that the low-field arrangement is a distorted spiral rather than a ferromagnet. At a critical field, the moments flop to a fan centered about the hard axis; and at a somewhat higher field, complete cancellation of the planar anisotropy is obtained.

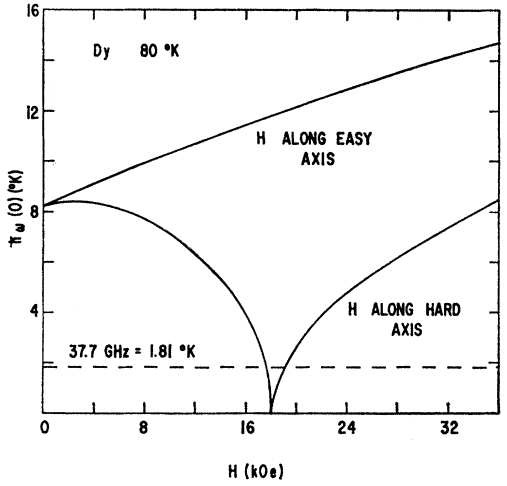

FIG. 7. Theoretical field dependence of $q=0$ spin-wave energy for Dy at 80°K when frozen-lattice approximation does not apply.

The detailed temperature dependence of the hard- and easy-axis resonance fields can be found using (4.9), in combination with (2.16), or (4.8), respectively, to calculate $\omega(0)$ as a function of H for a number of temperatures. We can first ask what would be expected if the frozen-lattice approximation were applicable with the values of D^γ and P_6^6 given by (6.5) and (6.6). The value of P_2 used is taken from the torque measurements of Rhyne and Clark.[5]

$$\text{Dy}, \quad P_2 S = -25.2°\text{K/atom}. \tag{7.2}$$

The results found at 80°K are shown in Fig. 6. As can be seen, the minimum value of $\hbar\omega(0)$ lies well above the energy equivalent of the signal frequency, 1.81°K. This is the typical behavior for all temperatures. Thus, the occurence of hard-axis resonant absorption strongly argues against the applicability of the frozen-lattice approximation.

We can also calculate the resonant-field behavior using the same values of P_2 and P_6, but putting $D^\gamma=0$ in (4.8) and (4.9), i.e., the case when the frozen-lattice approximation does not apply. Results of the calculation for 80°K, a typical case, are shown in Fig. 7. Because of the monotonic rise in $\hbar\omega(0)$ for H along the easy planar axis, one does not expect to observe resonance in that case. This is consistent with experiment. On the other hand, for H along a hard axis one expects to observe two closely spaced resonances where $\hbar\omega(0)$ matches the signal frequency. Actually, for the broad lines encountered, one could not expect to resolve the two separate resonances when they are only one or two kOe apart.

Detailed comparison between the calculated and experimental values of the hard-axis resonance for Dy are shown in Fig. 5. The two solid curves trace out the two values of H, as shown in Fig. 7 for 80°K, at which $\hbar\omega(0)$ equals the signal frequency, while the dashed curve gives the value of H for which $\hbar\omega(0)=0$. The experimental result agrees quite well with theory. This is especially true when we recall that the experimental value of P_6^6 found by Liu *et al.*[9] and used in our calculation may be somewhat high. (The value of Liu *et al.* exceeds that found by Rhyne and Clark[5,23] by about 40%.)

Hard-axis resonance experiments have also been performed in Tb by Bagguley and Liesegang.[8] Their results for the resonance field at 9.44 GHz are shown in Fig. 8. We have again used (4.9) to calculate the expected resonance frequencies. For the frozen-lattice case we use the same values of D^γ, P_6^6, and P_2 as were used to calculate the short-dashed "frozen-lattice" curve in Fig. 4. Again we find a situation similar to that illustrated in Fig. 3. Typically, the minimum value of $\omega(0)$ falls well above the energy equivalent of the signal frequency (0.45°K). For example, at 160°K the minimum value of $\hbar\omega(0)$ is 5.9°K (at 500 Oe). Thus, again for Tb as for Dy the observation of ferromagnetic-resonance absorption argues strongly against the applicability of the frozen-lattice approximation.

We have also calculated the hard-axis resonance field in Tb at 9.44 GHz using (4.9) with $D^\gamma=0$, choosing P_2 and P_6^6 to have the same values used in calculating the solid, "unstrained hexagonal anisotropy", curve in Fig. 4. As can be seen, the theoretical curves (the solid curves in Fig. 8) lie below the experimental values and drop off rather more sharply with increasing temperature.

Actually, as discussed in Sec. 6 (see Fig. 2) the hexagonal anisotropy in Tb may be largely associated with the magnetostriction rather than the hexagonal

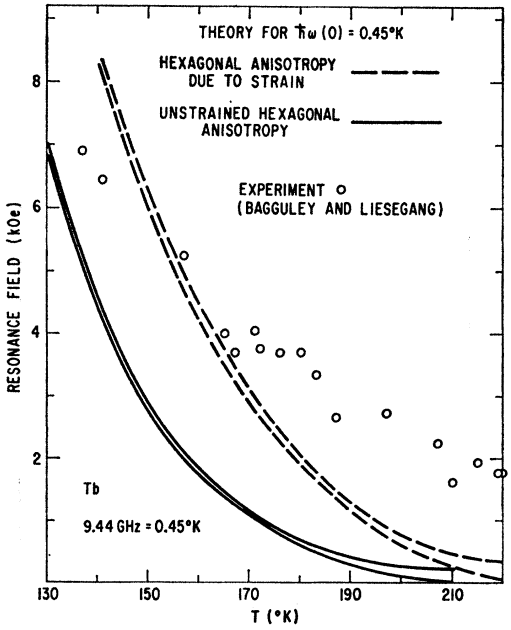

FIG. 8. Temperature dependence of resonance field in Tb at 9.44 GHz for H along a hard axis in the basal plane.

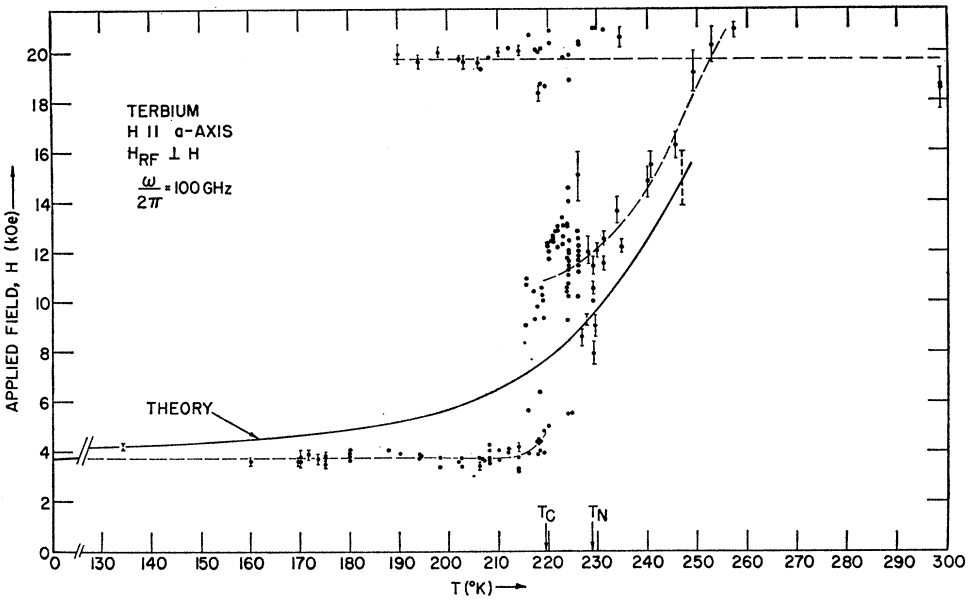

FIG. 9. Values of applied field for which power-absorption maxima occur in Tb at 100 GHz, plotted versus temperature [after J. S. Stanford and R. C. Young, Phys. Rev. **157**, 245 (1967)]. (The theoretical curve of Stanford and Young, which is also shown, involved some strong approximations and should be disregarded.)

anisotropy of the unstrained crystal. Using an equation similar to (5.12) [but including applied-field effects as in (2.17)] we have calculated the behavior of $\hbar\omega(0)$ when the hexagonal anisotropy has this origin. The results of this calculation are also shown in Fig. 8 (the dashed curves). The values of parameters used are the same as for the long-dashed, "hexagonal anisotropy due to strain," curve in Fig. 4. The experimental behavior agrees reasonably well with this theory at the lower temperatures shown in Fig. 8. However, for the higher temperatures shown, the experimental resonance field falls more slowly with increasing temperature than the theory would indicate. This may in part be due to the fact that the great width of the broad resonance line makes precise location of the peak difficult.

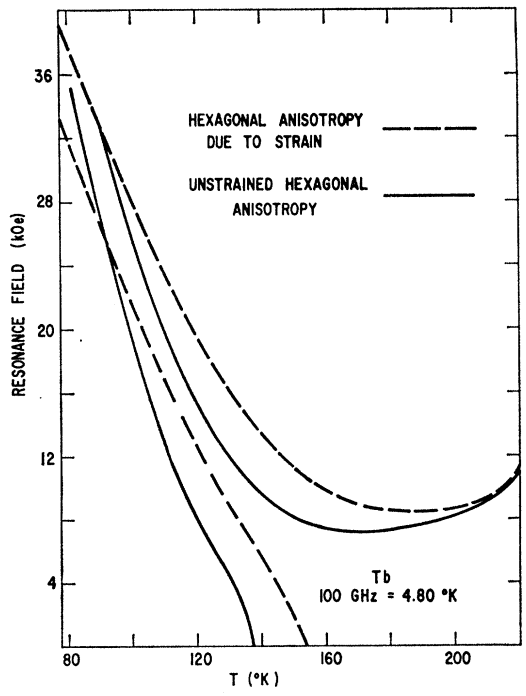

FIG. 10. Theoretical behavior expected for variation of resonance field with temperature for Tb at 100 GHz.

In contrast to the rather good agreement between the existing theory, when the frozen-lattice approximation is inapplicable, and experiment for the resonance experiments so far discussed (putting aside the question of the size of planar anisotropy in Tb), the experimental results of Stanford and Young[26] for Tb at 100 GHz are quite anomalous. The experimental results they obtained for the resonance field are shown in Fig. 9. (This is Fig. 4 of Stanford and Young. The theoretical curve shown involved some strong approximations and should be disregarded.) The applied dc field was along a hard planar axis. The results shown have several striking qualitative features.

There is a resonance line at about 3.8 kOe, the location of which is essentially temperature-independent between 160°K and the Curie temperature. The location of this resonance line breaks sharply upward at the Curie temperature. This is particularly striking because the critical field for the spiral to ferromagnetic transition in Tb is less than 1 kOe. Therefore, the fields used in the resonance experiment suppress the spiral between T_N and T_c. Presumably, however, the crystal still distorts at T_c because the decrease in crystal-field energy associated with the magnetostriction exceeds any increase in exchange energy associated with the distortion. Finally, there is a second resonance line at

[26] J. S. Stanford and R. C. Young, Phys. Rev. **157**, 245 (1967).

about 19 kOe, the location of which is approximately constant down to 190°K. (The two lines observed are very broad, so that resolving them below 190°K is impossible.)

The theoretical results expected for 100 GHz are shown in Fig. 10. The calculations have been done in exactly the same way, using the same values of parameters, as those shown in Fig. 8 for 9.44 GHz. Because of the increased frequency, the separation between the two fields at which $\hbar\omega(0)$ matches the signal frequency is decidedly greater than for 9.44 GHz. Thus, it might be possible to resolve two separate resonances in the hard-axis resonance experiment for some range of temperatures for either of the two approximations shown. However, for either approximation the lower of the two resonance fields varies quite strongly with temperature and goes to zero field at a temperature well below that of the observations of Stanford and Young. Thus, the observations of Stanford and Young are at variance with the existing theory. It is conceivable that some of the resonance effects observed may be caused by geometric effects and could be associated with the excitation of magnetostatic modes.

In this regard, it would be interesting to see if the observed behavior was sensitive to sample size. (The experiments[26] were performed on a flat disk approximately $\frac{3}{8}$ in. in diameter and having a diameter-to-thickness ratio of 4.2.) Also, it would be worth rotating the direction of the dc field to be along the easy axis. This would clarify the role played by hexagonal anisotropy in the behavior observed by Stanford and Young.

8. CONCLUSIONS

As discussed in the previous section, the results of neutron inelastic scattering experiments[6,7,7a] and of ferromagnetic-resonance experiments[8,10,11] point quite strongly to the conclusion that the frozen-lattice approximation for treating magnetoelastic effects on spin-wave energies is not applicable to Dy and Tb. Presumably the inapplicability of the frozen-lattice approximation is related to the low value of $\hbar\omega(0)$ relative to the Debye temperature. Vibrational modes are available whose frequencies are high compared with $\omega(0)$, so that the strain can accommodate itself to the instantaneous motion of the magnetization. It would be interesting to consider the intermediate case where some vestige of the frozen-lattice effect remains due to relaxation-time effects for the strain following the motion of the magnetization.

As already noted in the Introduction, the most striking point found in the present work is the contrast between the behavior of Dy and that of Tb with regard to understanding the long-wavelength spin-wave behavior using values of parameters for the anisotropy obtained from static macroscopic measurements. As shown in Fig. 5, for Dy one obtains very good agreement between the experimental values of the hard-axis ferromagnetic-resonance field and the results of an absolute calculation using the experimental value of the macroscopic planar anisotropy constant. On the other hand, for Tb the value of planar anisotropy constant necessary for agreement with the spin-wave experiments, both neutron scattering and ferromagnetic-resonance, is about four times that obtained in static measurements. It should be stressed that any mechanism intended to resolve the discrepancy between static and dynamic values of planar anisotropy in Tb should be consistent with the lack of any discrepancy in Dy.

ACKNOWLEDGMENTS

I am grateful to Miss E. Kreiger and Miss A. Warner for their assistance with the numerical calculations.